ELSEVIER

Journal of Nuclear Materials 298 (2001) 231–238

journal of nuclear materials

www.elsevier.com/locate/jnucmat

Accumulation of radioactive corrosion products on steel surfaces of VVER-type nuclear reactors. II. ^{60}Co

Kálmán Varga [a,*], Gábor Hirschberg [a], Zoltán Németh [a], Gerrit Myburg [b], János Schunk [c], Péter Tilky [c]

[a] *Department of Radiochemistry, University of Veszprém, P.O. Box 158, H-8201 Veszprém, Hungary*
[b] *Department of Physics, University of Pretoria, Pretoria, South Africa*
[c] *Paks NPP Co. Ltd., Paks, Hungary*

Received 5 March 2001; accepted 11 July 2001

Abstract

In the case of intact fuel claddings, the predominant source of radioactivity in the primary circuits of water-cooled nuclear reactors is the activation of corrosion products in the core. The most important corrosion product radionuclides in the primary coolant of pressurized water reactors (PWRs) are ^{60}Co, ^{58}Co, ^{51}Cr, ^{54}Mn, ^{59}Fe (as well as ^{110m}Ag in some Soviet-made VVER-type reactor). The second part of this series is focused on the complex studies of the formation and build-up of ^{60}Co-containing species on an austenitic stainless steel type 08X18H10T (GOST 5632-61) and magnetite-covered carbon steel often to be used in Soviet-planned VVERs. The kinetics and mechanism of the cobalt accumulation were studied by a combination (coupling) of an in situ radiotracer method and voltammetry in a model solution of the primary circuit coolant. In addition, independent techniques such as X-ray photoelectron spectroscopic (XPS) and ICP-OES are also used to analyze the chemical state of Co species in the passive layer formed on stainless steel as well as the chemical composition of model solution. The experimental results have revealed that: (i) The passive behavior of the austenitic stainless steel at open-circuit conditions, the slightly alkaline pH and the reducing water chemistry can be considered to be optimal to minimize the ^{60}Co contamination. (ii) The highly potential dependent deposition of various Co-oxides at $E > 1.10$ V (vs. RHE) offers a unique possibility to elaborate a novel electrochemical method for the decrease or removal of cobalt traces from borate-containing coolants contaminated with ^{60}Co and/or ^{58}Co radionuclides.

PACS: 82.55.+e; 81.65.Kn; 79.60.Ht

1. Introduction

It is well known that in the primary circuit of water-cooled nuclear reactors there are three main sources of the radioactive contamination: (a) fission products and actinides released from faulty fuel elements; (b) activation of feed water and its impurities; (c) activation of various corrosion products [1,2]. Under normal operating conditions (when there is no fission product release due to fuel cladding failure) the majority of radioactive contamination in the primary loop are caused by various radioactive corrosion products. The most important corrosion product radionuclides in the primary side coolant of pressurized water reactors (PWRs) are ^{60}Co, ^{58}Co, ^{51}Cr, ^{54}Mn, ^{59}Fe (as well as ^{110m}Ag in some Soviet-made VVER-type reactor) ([3–9] and references cited therein). The two cobalt isotopes are known to be the predominant contaminants, but the ^{60}Co bears a special importance owing to its relatively long half-life (5.27 years) and high-energy γ-photons (1.17 and 1.33 MeV). These two factors work towards ^{60}Co causing up to 80% of the radiation exposure to the reactor operating personnel. Thus, it is no wonder that the formation and accumulation of cobalt on different surfaces and under

* Corresponding author. Fax: +36-88 427 681.
E-mail address: vargakl@almos.vein.hu (K. Varga).

0022-3115/01/$ - see front matter
PII: S0022-3115(01)00658-4

various conditions have been the scope of many studies so far (see e.g., [3–8] and references cited therein). In spite of the great effort put out by both Western and Eastern research groups, many issues of cobalt contamination are still open to debate. It can easily be understood that knowledge of the fundamental aspects of cobalt deposition is needed, which may facilitate the elaboration of more efficient surface prevention and/or decontamination procedures.

The aim of the second part of this series is therefore to present some findings obtained by the in situ radiotracer, voltammetric and X-ray photoelectron spectroscopic (XPS) studies of cobalt accumulation on austenitic stainless steel type 08X18H10T (GOST 5632-61) and magnetite-covered carbon steel surfaces. In addition, we report some preliminary results measured in a semi-plant model system by making use of an ex situ radiotracer method and ICP optical emission spectrometry in order to demonstrate the potentialities of a novel electrochemical method for the decrease or removal of cobalt traces from borate-containing coolants.

2. Experimental section

2.1. In situ radiotracer, voltammetric and XPS studies

The in situ radiotracer experiments, aimed to study the kinetics and mechanism of cobalt contamination on steel surfaces, were conducted following the same protocol described in our previous papers [8,9]. All the equipments (including the XPS instrument utilized), chemicals and specimens were identical with those applied earlier [9]. The additional voltammetric measurements were carried out by a VoltaLab 40 (Radiometer)-type electrochemical measuring system controlled by PC.

All the experiments were carried out at room temperature in a model solution of the primary cooling circuit of VVER-type nuclear reactors. (The composition of this solution is tabulated in Table 1.) Disk-shaped electrodes (diameter: 10.0 mm; thickness: 2–3 mm) were cut from austenitic stainless steel type 08X18H10T (GOST 5632-61) and magnetite-covered carbon steel. The stainless steel samples (5 specimens) were polished to optical quality with emery paper and diamond paste (down to 0.25 μm), while the magnetite-covered ones (2 specimens) were polished only very slightly in order to save the magnetite layer. The prepared specimens were degreased with ethanol, washed with Millipore water and introduced in to the radioelectrochemical cell of the in situ electrode-lowering method [8,9].

Table 1
The composition of the model solution ($pH_{25\ ^\circ C} \cong 7.7$)

Component	Concentration (g kg^{-1})
H_3BO_3	3
KOH	5.2×10^{-3}
NaOH	0.4×10^{-3}
LiOH	3.2×10^{-3}
NH_3	30×10^{-3}
N_2H_4	0.02×10^{-3}
O_2	$<0.02 \times 10^{-3}$
Cl^-, SO_4^{2-}	$<0.05 \times 10^{-3}$

The ^{60}Co isotope was purchased from Izinta, Hungary having a molar activity of 3.3×10^{12} Bq mol^{-1}. Characteristic properties of the isotope are listed in Table 2 [10]. Throughout the experiments the cobalt concentration was set to 1×10^{-6} mol dm^{-3} in the solution phase. The surface amount of sorbed cobalt species was calculated from the intensity of the β-radiation emitted by ^{60}Co ($E_{\beta max} = 318$ keV) by making use of the following relationship [8,9]:

$$\Gamma = \frac{I_A c}{I_B \mu \gamma f_b \exp(-\mu x)}, \quad (1)$$

where Γ is the surface excess of sorbed Co species (mol cm^{-2}) i.e., the g-moles of Co-containing species adsorbed on 1 cm^2, I_A: counting rate proportional to the amount of Co species adsorbed on the working electrode (cpm), I_B: counting rate originating from the bulk solution (cpm), c: solution concentration (mol cm^{-3}), μ: linear attenuation coefficient for β-radiation of ^{60}Co in dilute water solution ($\mu = 66.5$ cm^{-1}, [11]), f_b: measured value of the saturation backscattering factor ($f_{b,austenitic} = 1.25$; $f_{b,magn} = 1.30$), x: actual thickness of the solution gap (cm), γ: roughness factor of the electrode surface. Due to the lack of an appropriate method to determine the real surface area of the steel electrodes (i.e., to calculate the roughness factor of the electrode surface (γ)), we provide the surface excess data as a product of $\Gamma\gamma$. All the potential values quoted in this paper are on the reference hydrogen electrode (RHE) scale.

2.2. Experiments in semi-plant model system

In the knowledge of the selective deposition processes of Co-oxides at potentials above 1.10 V, a column-like semi-plant adsorption system was elaborated for the purification of borate-containing coolants

Table 2
Characterizing features of the ^{60}Co radioisotope

Half-life (year)	E_γ (MeV)	Probability (%)	$E_{\beta max}$ (MeV)	Probability (%)
5.28	0.694	0.02	0.318	100
	1.173	100		
	1.332	100		

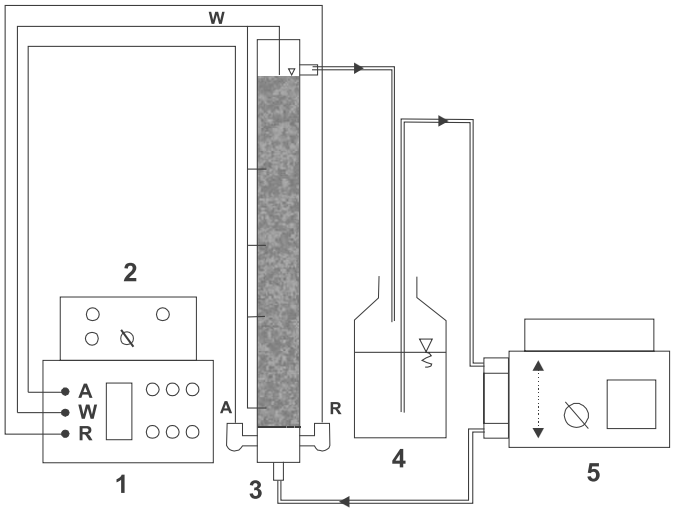

Fig. 1. Schematic of the semi-plant purification system. (1) Potentiostat; (2) Function generator; (3) Adsorption column filled up with stainless steel splints; (4) Glass container for the model solution; (5) Peristaltic pump. (Electrodes: A: auxiliary; R: reference; W: working)

contaminated with ^{60}Co and/or ^{58}Co radionuclides. As may be seen from Fig. 1, this decontamination system consists of an adsorption column filled up with stainless steel splints having a geometric surface area of about 3200 cm^2, a peristaltic pump, a glass container for 5 dm^3 model solution labeled with ^{60}Co and silicone rubber piping. The surface of the stainless steel splints in the column had undergone cyclic polarization in the potential range 1.00–1.60 V (vs. RHE) using an EF-421-type potentiostat and an EF-1808-type function generator (both made by Electroflex, Hungary). The model solution contaminated with ^{60}Co ($c_{\mathrm{Co(II)}} = 1 \times 10^{-7}$ mol dm^{-3}) went through the column continuously and the cobalt concentration was analyzed chronologically by measuring the intensity of the γ-radiation of 20 cm^3 solution samples. For the measurement of γ-photons a Canberra-type HpGe semiconductor detector attached to a multi-channel pulse-height analyzer (PCA-Multiport 8k, Oxford Inc., USA) was applied. In addition, the concentration of various metals dissolved from the stainless steel splints into the solution was studied by ICP optical emission spectrometry (type of spectrometer: ICP Thermo Jarrell Ash ICAP 61E).

3. Results and discussion

3.1. Voltammetric, in situ radiotracer and XPS studies of Co accumulation

As mentioned in Section 2, the measurements were carried out in the same sequence as before in the case of the ^{110m}Ag [9]. First the voltammetric behavior of the steel sample/borate buffer solution interface was studied. Fig. 2 shows the potentiostatic polarization curves of the austenitic stainless steel in a model solution of primary coolant in the absence and presence of Co(II) species. The current density vs. potential curves in Fig. 2 are in accordance with the cyclic voltammograms presented in [9], and reveal that the austenitic stainless steel exhibits passive properties in a wide potential range (up to 1.10 V), including the corrosion potential. Addition of cobalt species to the solution phase does not exert any significant effect on the shape of the above voltammograms in the passivity region up to the concentration of 1×10^{-5} mol dm^{-3}.

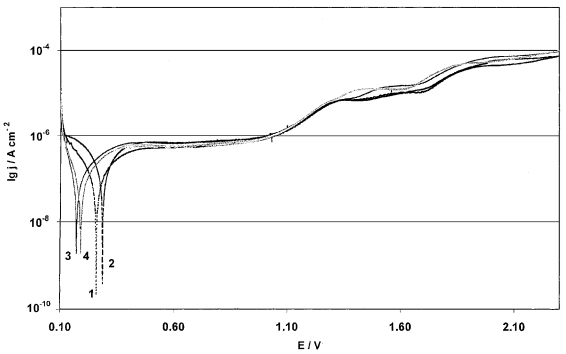

Fig. 2. Potentiostatic polarization curves of austenitic stainless steel type 08X18H10T (GOST 5632-61) in a model solution of primary side coolant at various Co(II) concentrations: (1) 0; (2) 1×10^{-7}; (3) 1×10^{-6}; (4) 1×10^{-5} mol dm^{-3}. Scan rate: 0.166 mV s^{-1}.

Voltammetric features of magnetite-covered carbon steel in borate buffer solution both in the absence and presence of Co(II) species are identical with those reported earlier (see Fig. 5 in [9]). Namely, an active dissolution of the carbon steel proceeds at the above potentials to yield surface covered by more and more corrosion products.

In the light of the voltammetric measurements, the accumulation of cobalt species (labeled by ^{60}Co) was studied on steel surfaces by the in situ electrode-lowering radiotracer method.

In Fig. 3 the time dependence of cobalt sorption can be seen at austenitic stainless steel type 08X18H10T (GOST 5632-61) surface. The sorption exhibits saturation feature after about 20 h, although the amount of cobalt accumulated on the surface is extremely low. The maximum surface excess measured was about 2.5×10^{-12} mol cm^{-2} which is approximately 0.5% of a monolayer coverage calculated assuming close packing of the cobalt hydrolysis products ($\Gamma_{ML} = 4.3 \times 10^{-10}$ mol cm^{-2}) [12]. In spite of the low level of contamination, the parallel measurements performed on different stainless steel specimens reveal good reproducibility of the Γ values. A verification of this statement is given by the Γ vs. time curves obtained in three parallel experiments (see the inset to Fig. 3). The 20% difference in the Γ values may most likely be attributed to the different roughness factors of the given steel samples.

Potential dependence results of cobalt contamination on austenitic stainless steel are shown in Fig. 4 (the surface excess values depicted in this figure were measured after 30 min contamination period). In the potential range −0.10 to 1.10 V (the passive region of this steel sample) only slight changes in the surface excess can be observed (curves 1, 2 and 2′). On the negative-going branch one may see a minor increase in the Γ values. It may be the result of the reduction of oxygen traces to OH^- ($O_2 + 2H_2O + 4e^- = 4OH^-$), which promotes the formation of cobalt hydrolysis products possessing much higher sorption ability than the Co^{2+} ions. (Later, we shall give a more detailed explanation for the above-mentioned phenomenon.) In these laboratory-scale investigations the inert gas (high-purity argon) bubbling through the solution removes the vast majority of the dissolved oxygen from the solution, while in a PWR-type nuclear reactor the reducing water chemistry (addition of NH_3 and/or N_2H_4) may help to overcome this problem.

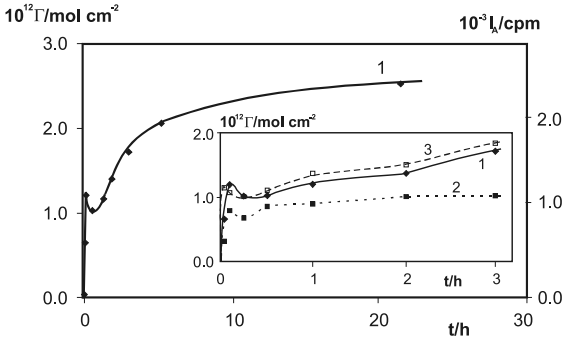

Fig. 3. Time dependence of ^{60}Co sorption on austenitic stainless steel in the model solution at open-circuit potential. Curves 1–3 in the inset were obtained under identical experimental conditions on three parallel (different) steel samples. Open-circuit potential values are 0.84 (curves 1 and 3) and 0.83 (curve 2).

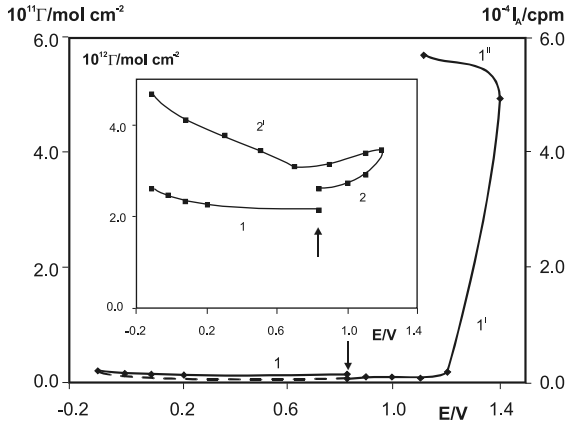

Fig. 4. Potential dependence of ^{60}Co sorption on austenitic stainless steel in model solution containing 1×10^{-6} mol dm^{-3} Co(II). Arrows indicate the open-circuit potential values. Curve 1: polarization into negative direction starting from open-circuit potential ($E = 0.83$ V). Curve 1′: after negative polarization potential was set to $E = 0.83$ V and polarization into positive direction. Curve 1″: finishing polarization after reaching $E = 1.40$ V. Curve 2: polarization into positive direction starting from open-circuit potential ($E = 0.84$ V). Curve 2′: polarization into negative direction after reaching $E = 1.20$ V.

Interesting potential dependence results were obtained upon polarizing the austenitic steel surface above 1.10 V. The corresponding curves are 1′ and 1″ in Fig. 4. During a period of 30 min the surface excess values increased by one and half orders of magnitude and kept on growing upon cathodic polarization too. This conspicuous behavior was investigated in separate voltradiometric experiments in the course of the continuous cyclic polarization of the sample in the range 1.10–1.40 V. The resulting curves are depicted in Fig. 5. It is clear from the curves that: (i) the cobalt layer is growing continuously on the surface, (ii) the bigger the cobalt amount on the surface, the bigger the cobalt intake during the cathodic-going polarization. Similar findings were reported by Varga and Kolics [13] on polycrystalline gold surface in a borate buffer solution. Therefore, the potential dependent depositions of cobalt above $E = 1.10$ V are almost identical on a noble metal and on

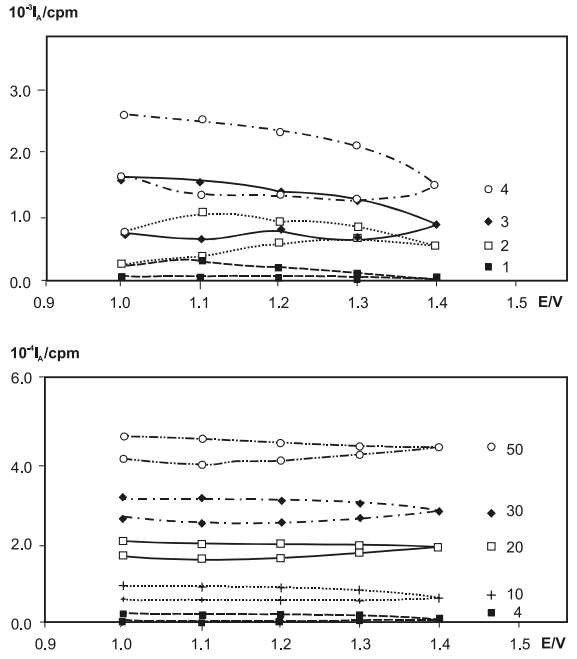

Fig. 5. Accumulation of ^{60}Co on austenitic stainless steel from model solution containing 1×10^{-6} mol dm^{-3} Co(II) upon cyclic polarization in the range 1.0–1.4 V vs. RHE. Arabic numbers beside the curves correspond to the number of cycles. Scan rate: 10 mV s^{-1}.

a stainless steel surface (which is in a transpassive state), giving a strong indication of the unique sorption feature of the cobalt species rather than the surfaces studied. Moreover, it should be noted that such a phenomenon has only been experienced in solutions containing borate species, however, the exact role of borate ions (and complexes) in this process is not clear at the moment [13,14].

Considering the potential diagram of Co-containing species at pH = 7.7 (see Fig. 6) the possible mechanism of the high cobalt deposition found above 1.10 V is as follows [8,13]:

1. The oxidation of previously deposited Co(II) species to Co(IV) may proceed at anodic potentials according to the following equations:

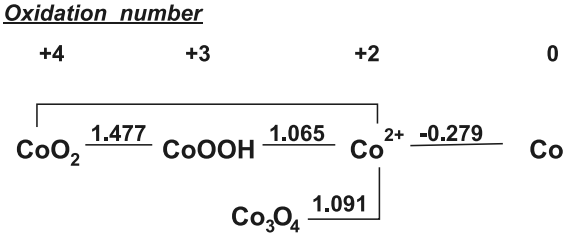

Fig. 6. Potential diagram of Co-containing species at pH = 7.7.

- Formation of Co(III)-oxide:

$$Co^{2+} + 2H_2O \Longleftrightarrow CoOOH + 3H^+ + e^- \quad (2)$$

$$3Co^{2+} + 4H_2O \Longleftrightarrow Co_3O_4 + 8H^+ + 2e^- \quad (3)$$

$$3Co(OH)_2 \Longleftrightarrow Co_3O_4 + 2H^+ + 2H_2O + 2e^- \quad (4)$$

$$Co_3O_4 + 2H_2O \Longleftrightarrow 3CoOOH + H^+ + e^-. \quad (5)$$

- Formation of Co(IV)-oxide:

$$Co^{2+} + 2H_2O \Longleftrightarrow CoO_2 + 4H^+ + 2e^- \quad (6)$$

$$CoOOH \Longleftrightarrow CoO_2 + H^+ + e^-. \quad (7)$$

2. The reduction of Co(IV) in the course of the cathodic-going polarization is coupled with the build-up of Co^{2+} ions from the solution phase in the range 1.00–1.60 V (embedding of Co(II) into the surface Co-oxide layer):

$$2CoO_2 + Co^{2+} + 2e^- \Longleftrightarrow Co_3O_4. \quad (8)$$

In order to give a verification of the above mechanism, i.e., to characterize the chemical state and depth profile of the cobalt in the passive oxide layer of the steel sample XPS experiments were carried out. For this purpose 20×20 mm rectangular samples of the austenitic stainless steel type 08X18H10T (GOST 5632-61) were polarized continuously in the potential range 1.0–1.4 V in the model solution containing 1×10^{-6} mol dm^{-3} inactive Co(II). Cobalt was found in trace amounts (~0.2%) only on the sample surface, which was cyclically polarized in the above-mentioned potential range for 2000 times. This very small amount of surface Co species made it impossible to acquire chemical information about the deposited cobalt. Fig. 7 shows the Co2p3 peak recorded during Ar-ion sputtering. As can be seen from this figure, the cobalt peak overlaps with the LMM Auger-transition of iron; the wide and intensive Auger-peak hinders the resolution and decomposition of the cobalt peak. It is, however, interesting to compare the detection limits of the XPS measurements and the radiotracer electrode-lowering method. Fig. 5 clearly shows that in the radiotracer experiment 50 polarization cycles caused a significant intensity surplus as high as 50 000 cpm.

The comparative measurements shown in Fig. 8 reveal that the cobalt accumulation on magnetite-covered carbon steel from model solution under open-circuit conditions is two orders of magnitude higher than on austenitic stainless steel. Moreover, the Γ vs. time curve does not show the equilibrium feature and the cobalt deposition is very intensive even after 17 h. Polarizing the surface in the potential region of −0.1 to 1.1 V (starting from the open-circuit potential) the amount of cobalt continuously decreases (see Fig. 9), which is the contrary of the behavior found at the austenitic stainless

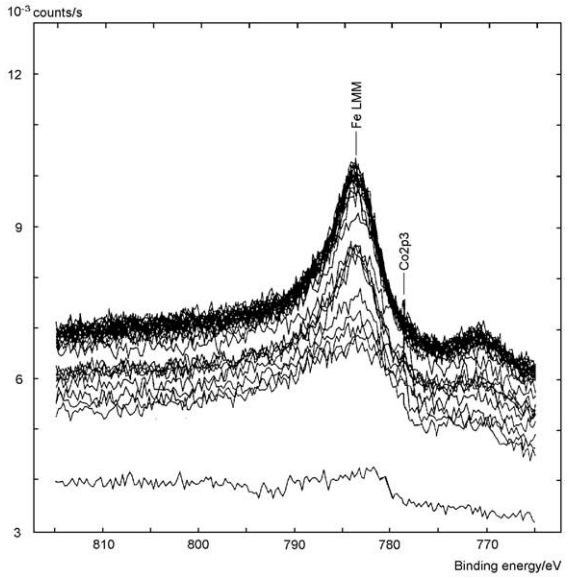

Fig. 7. XPS scans of the FeLMM Auger-peak of austenitic stainless steel sample after 2000 polarization cycles in the potential region of 1.0–1.4 V in model solution containing 1×10^{-6} mol dm^{-3} unlabeled Co(II).

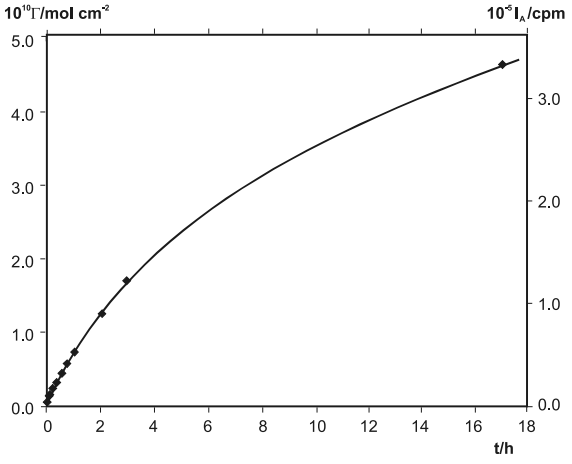

Fig. 8. Time dependence of Co sorption on magnetite-covered carbon steel in model solution under open-circuit ($E = 0.37$ V) conditions.

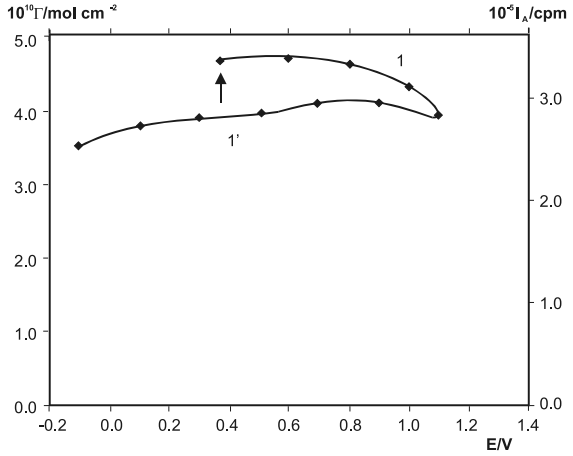

Fig. 9. Potential dependence of Co sorption on magnetite-covered carbon steel in model solution containing 1×10^{-6} mol dm^{-3} Co(II). Arrow indicates the open-circuit potential ($E = 0.37$ V). Curve 1: polarization from open-circuit potential to 1.1 V. Curve 1′: polarization from 1.1 to −0.1 V.

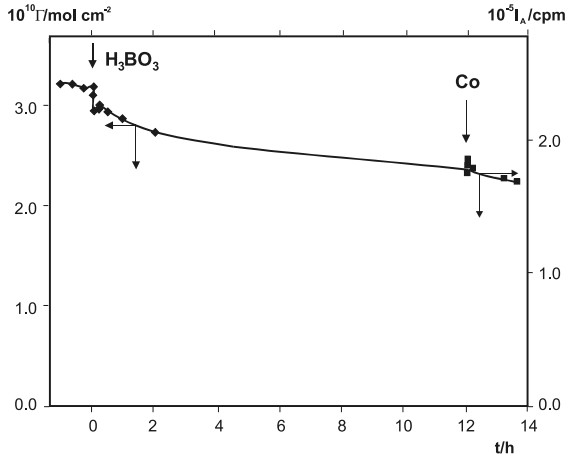

Fig. 10. Study of the mobility of ^{60}Co adsorbed on magnetite-covered carbon steel upon the increase of boric acid concentration up to 13 g dm^{-3} and the addition of inactive cobalt in great excess (10^{-4} mol dm^{-3}). Arrows indicate the moment of addition.

steel surface. The mobility study in Fig. 10 shows that it is also impossible to mobilize the deposited cobalt either by addition of boric acid or by great excess of inactive Co(II). The latter effect is indicative of the strong embedding of the cobalt species into the surface oxide layer of the sample.

The conspicuous behavior of Co accumulation on magnetite-covered carbon steel may be explained by considering two factors: (i) the distribution and relative adsorbability of the hydrolysis products of Co(II) at $c_{Co} < 1 \times 10^{-5}$ mol dm^{-3}, and (ii) the active dissolution of carbon steel surface in the entire potential region studied.

The relative proportion of different Co(II) species as a function of the pH of the borate buffer solution, calculated on the basis of data reported in [15], is depicted in Fig. 11. At lower pH values, up to about pH = 7.5, Co^{2+} ions are present mostly in the solution. Above this value various hydrolysis products such as $CoOH^+$,

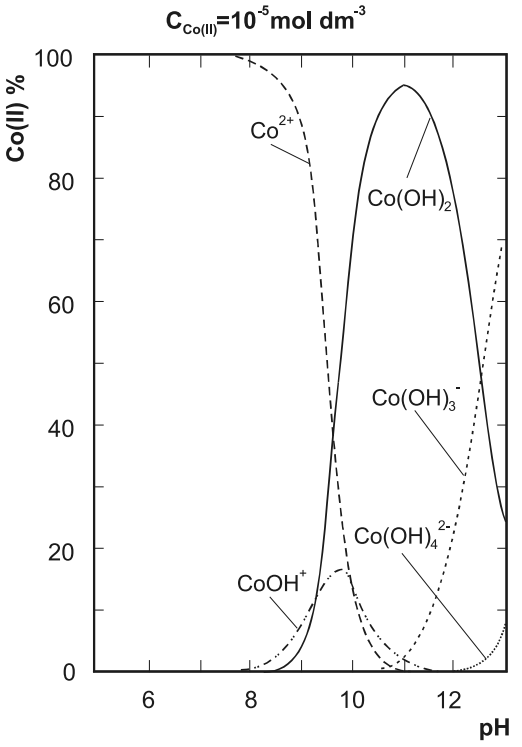

Fig. 11. Distribution of Co(II) hydrolysis products as a function of the pH in the model solution at 25 °C. Equilibrium relationships were calculated on the basis of the data reported in [15].

$Co(OH)_2$, $Co(OH)_3^-$, $Co(OH)_4^{2-}$ tend to be formed. As has been pointed out in various laboratories (e.g., [3–8, 12–18]), the sorption ability of $CoOH^+$ and $Co(OH)_2$ is significantly higher than that of Co^{2+}. Also, the literature data (see e.g., [3–8,16,17] and references therein) testify that on various iron oxides at pH > 8.0 the cobalt contamination increases. However, when the formation of $Co(OH)_3^-$ and $Co(OH)_4^{2-}$ starts to take place, the surface excess of cobalt decreases, because the solubility of these hydrolysis products is higher than that of $Co(OH)_2$.

Therefore, the high rate of cobalt deposition on the magnetite-covered carbon steel may most likely be attributed to the effects of the heavily corroding and transforming carbon steel base metal. Namely, the corrosion products being formed and dissolved into the solution phase facilitate the formation of the cobalt hydrolysis products ($CoOH^+$ and $Co(OH)_2$) in borate solution (owing to the change in the local pH near the steel surface), which most likely accumulate at and embed into the oxide layer. Also, the continuous roughening of the steel surface as a consequence of the intense corrosion processes provides favorable conditions for extensive cobalt accumulation.

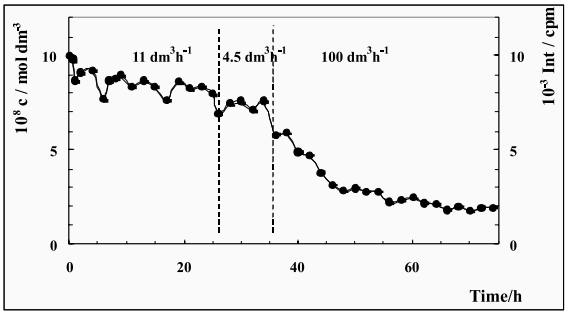

Fig. 12. Time dependence of the solution concentration and intensity of radioactive cobalt species measured at various volume rates in the course of the decontamination of a model solution of the primary side coolant in semi-plant purification system.

3.2. An attempt for the decontamination of primary coolant in semi-plant model system

In the light of the selective deposition processes of Co-oxides on austenitic stainless steel at potentials above 1.10 V, experiments were performed in a column-like semi-plant adsorption system (Fig. 1) elaborated for the purification of borate-containing coolants contaminated with ^{60}Co and/or ^{58}Co radionuclides. We attempted to study the change in the solution concentration (and activity) of Co isotopes as a function of various parameters (such as time, polarization rate, polarization region, volume rate of coolant pumped through the column, formation and geometric surface area of the stainless steel adsorbent). Fig. 12 shows some preliminary results of the time dependence of the selective decontamination of ^{60}Co containing solutions obtained under experimental conditions detailed in Section 2. As demonstrated in Fig. 12, a significant part (up to 80%) of the total amount (and activity) of ^{60}Co can be removed from the coolant within a period of 60 h. It should be highlighted here that the concentrations of various metals dissolved from the steel splints into solution during the treatment were found to be under the detection limit of the ICP-OES method ($c_{Cr,Fe} < 0.01$ mg dm^{-3}, $c_{Mn} < 0.02$ mg dm^{-3}, $c_{Ni} < 0.03$ mg dm^{-3}). All these data give further verification of the mechanism proposed by Eqs. (2)–(8).

4. Conclusion

The results of the laboratory-scale studies carried out using a combination of the in situ radiotracer electrode-lowering method and voltammetry underlined the importance of the strict control of operating parameters in water-cooled nuclear reactors. It has been found that: (i) The passive behavior of the austenitic stainless steel at

open-circuit conditions, the slightly alkaline pH and the reducing water chemistry can be considered to be optimal to minimize the ^{60}Co contamination. (ii) The highly potential dependent deposition of various Co-oxides at $E > 1.10$ V offers a unique possibility to elaborate a novel electrochemical method for the decrease or removal of cobalt traces from borate-containing coolants contaminated with ^{60}Co and/or ^{58}Co radionuclides.

The column-like adsorption system elaborated for the semi-plant decontamination of primary side coolants provides very promising preliminary results, however, the optimization of the experimental conditions requires further investigations.

Acknowledgements

This work was supported by the Paks NPP Co. Ltd. (Paks, Hungary), the Hungarian Science Foundation (OTKA Grant No. 31971) and the Ministry of Education of Hungary (Grant No. 0789/97).

References

[1] G. Choppin, J. Rydberg, J.O. Liljenzin, Radiochemistry and Nuclear Chemistry, Butterworth–Heinemann, Oxford, 1995.
[2] D. Bodansky, Nuclear Energy–Principles Practices and Prospects, AIP, Woodbury, NY, 1996.
[3] D.H. Lister, Water Chem. Nucl. React. Systems, 6. BNES, London, 1992, p. 49.
[4] G.C.W. Comley, Prog. Nucl. Energy 16 (1985) 41.
[5] A.P. Murray, Nucl. Technol. 74 (1986) 324.
[6] G. Romeo, Characterization of corrosion products on recirculation and bypass lines at Millstone-1, Research Project 819-1, EPRI NP-949, Interim Report, 1978.
[7] Proceedings of the Third International Seminar on Primary and Secondary Side Water Chemistry of Nuclear Power Plants, Balatonfüred, Hungary, September 16–20, 1997.
[8] K. Varga, G. Hirschberg, P. Baradlai, M. Nagy, in: E. Matijevic (Ed.), Surface and Colloid Science, vol. 16, Plenum, New York, 2001, p. 341.
[9] G. Hirschberg, P. Baradlai, K. Varga, G. Myburg, J. Schunk, P. Tilky, P. Stoddart, J. Nucl. Mater. 265 (1999) 273.
[10] R.B. Firestone, in: V.S. Shirley (Ed.), Table of Isotopes, Wiley, New York, 1996.
[11] A. Vértes, I. Kiss. In: Nuclear Chemistry, Elsevier, Amsterdam, 1987, p. 118.
[12] R.O. James, T.W. Healy, J. Colloid Interf. Sci. 47 (1972) 65.
[13] A. Kolics, K. Varga, Electrochim. Acta 40 (1995) 1835.
[14] A. Kolics, K. Varga, J. Colloid Interf. Sci. 168 (1994) 451.
[15] C.F. Baes, R.E. Mesmer, The Hydrolysis of Cations, Wiley, New York, 1976.
[16] H. Tamura, E. Matijevic, L. Meites, J. Colloid Interf. Sci. 92 (1982) 303.
[17] A. Kolics, K. Varga, E. Maleczki, E. Házi, G. Horányi, Magy. Kém. Folyóirat 96 (1990) 296.
[18] H. Tamura, N. Katayama, R. Furuichi, J. Colloid Interf. Sci. 195 (1997) 192.